# DETECTION AND LOCALIZATION FOR AN UNKNOWN EMITTER USING TDOA MEASUREMENTS AND SPARSITY OF RECEIVED SIGNALS IN A SYNCHRONIZED WIRELESS SENSOR NETWORK

*Shaokan Zhang*[†]*, Huijuan Jiang*[‡]*, and Kehu Yang*[†]

[†] ISN Lab, Xidian University
South Taibai Road #2, 710071, Xi'an, China
[‡] Nanjing Telecommunication Technology Institute
No.18, houbiaoying Road, baixia District, 210007, Nanjing, China
Email: [†]zhangshaokan@gmail.com, yang001@xidian.edu.cn, [‡] littlejhj@163.com

**ABSTRACT**

We consider the problem of detection and localization for an unknown emitter in a synchronized wireless sensor network. The detection is investigated by the classical binary Bayesian hypothesis testing using TDOA measurements and the localization is tackled in the framework of support detection with the joint TDOA information and sparsity of the receiving signal. We derive the decision rule with TDOA measurements by multiple synchronized sensor nodes and simultaneously the decision threshold under the given constant false alarm (CFAR) probability according to the Neyman-Pearson principle. In the framework of support detection, we propose that the TDOA-based localization and detection could be performed in the manner similar to radar by using range cells. Simulation results show that both the proposed methods are effective in the detection and localization of an unknown emitter.

***Index Terms*—** Detection and Localization, TDOA, support detection, sensor network

## 1. INTRODUCTION

It is known that detection, localization, and tracking (DLT) of an unknown emitter is one of the important tasks in civilian and military applications. With multiple sensor nodes synchronized in a wireless sensor network (WSN), the DLT can be respectively performed by employing either the peak amplitude of the multiple pairwise crosscorrelation of the received signals at multiple sensor nodes or their corresponding time difference of arrival (TDOA) [1] and frequency difference of arrival (FDOA), or both.

In order to reduce excessive data transmission among the associated nodes and its resulted additional delay, distributed detection are often considered [2, 3]. It has been shown that when the signals received by the associated sensor nodes are correlated, the local optimal decision rules [3] for each sensor node do not have the explicit form comparing with that of the likelihood ratio threshold when the received signals are independent, and solving the local optimal decision rules becomes an NP-complete problem [2]. However, for the case of detecting and localizing an unknown emitter using TDOA measurements, it is necessary to perform pairwise crosscorrelation among the synchronized sensor nodes, which at least requires one sensor node, or called a cluster head to broadcast its received signals to its neighboring ones. The detection and localization can be performed at the cluster head according to the TDOA measurements fed back from these neighboring nodes.

Recently, sparse signal processing shares its light in many application areas [4][5]. With respect to the considerable area surveyed by a wireless sensor network, unknown emitters are always sparse in space. This sparsity can be exploited for detection and localization under the framework of support detection in sparse signal processing [4][5].

In this paper, we focus on the detection and localization using TDOA measurements and sparsity of the received signals and propose the TDOA-based detection and localization under the framework of support detection.

## 2. PROBLEM FORMULATION

### 2.1. Signal Model

Consider a scenario whereby a network of passive sensors collaborate to detect an unknown emitter. The locations of the sensor nodes are assumed to be known. In the ensuing mathematical formulation, we adopt the following notations: $t_j$ is the signal propagation delay from the emitter to the $j$th sensor node; $\boldsymbol{u} \in \mathcal{R}^3$ is the location of the unknown emitter to be detected; $M$ is the number of sensor nodes; $\boldsymbol{s}_j$ is the location of $j$th sensor node; $c$ is the speed of light. Assuming line-of-sight signal propagation, the TDOA measurements can be obtained by pairwise crosscorrelation of the received signals at multiple synchronized sensor nodes and is denoted by

$$\tau_{ij} = \frac{1}{c}\|\boldsymbol{u} - \boldsymbol{s}_i\| - \frac{1}{c}\|\boldsymbol{u} - \boldsymbol{s}_j\| + n_{ij}, \quad i \neq j \tag{1}$$

where $i, j = 1, \ldots, M$, and $n_{ij}$ is the measurement noise. In the case of pairwise crosscorrelation, the independent TDOA measurements are often denoted by

$$\boldsymbol{\tau} = [\tau_{21}, \tau_{31}, \ldots, \tau_{M1}]^T \tag{2}$$

where the first node is considered as the reference one, and the corresponding measurement noise vector is denoted by

$$\boldsymbol{n} = [n_{21}, \ldots, n_{M1}]^T \tag{3}$$

where $\boldsymbol{n}$ is often assumed to obey Gaussian distribution with zero mean and the covariance matrix $\boldsymbol{Q}$ [6].

### 2.2. Detection Using TDOA Measurements

The binary hypothesis testing problem [3] using TDOA measurements can be represented by

$$\begin{aligned} &H_0 : \boldsymbol{\tau} = \boldsymbol{n}, \\ &H_1 : \boldsymbol{\tau} = \tilde{\boldsymbol{\tau}} + \boldsymbol{n} \end{aligned} \tag{4}$$

where

$$\tilde{\boldsymbol{\tau}} = \begin{bmatrix} \frac{1}{c}\|\boldsymbol{u}-\boldsymbol{s}_2\| - \frac{1}{c}\|\boldsymbol{u}-\boldsymbol{s}_1\| \\ \frac{1}{c}\|\boldsymbol{u}-\boldsymbol{s}_3\| - \frac{1}{c}\|\boldsymbol{u}-\boldsymbol{s}_1\| \\ \vdots \\ \frac{1}{c}\|\boldsymbol{u}-\boldsymbol{s}_M\| - \frac{1}{c}\|\boldsymbol{u}-\boldsymbol{s}_1\| \end{bmatrix}. \tag{5}$$

It is evident to see that

$$\begin{aligned} &p(\boldsymbol{\tau}|H_0) \sim \mathcal{N}(\boldsymbol{0}, \boldsymbol{Q}), \\ &p(\boldsymbol{\tau}|H_1) \sim \mathcal{N}(\tilde{\boldsymbol{\tau}}, \boldsymbol{Q}). \end{aligned} \tag{6}$$

The corresponding likelihood ratio test (LRT) is denoted by

$$l(\boldsymbol{\tau}) = \frac{p(\boldsymbol{\tau}|H_1)}{p(\boldsymbol{\tau}|H_0)} \underset{H_0}{\overset{H_1}{\gtrless}} \eta \tag{7}$$

where the threshold $\eta$ is often chosen according to the specified false alarm probability

$$P_F = P(H_1|H_0) = \int_{Z_1} p(\boldsymbol{\tau}|H_0) d\boldsymbol{\tau}. \tag{8}$$

Here $Z_1$ denotes the decision region corresponding to hypothesis $H_1$. Therefore, the probability of detection can be obtained by

$$P_D = P(H_1|H_1) = \int_{Z_1} p(\boldsymbol{\tau}|H_1) d\boldsymbol{\tau}. \tag{9}$$

According to the distribution assumption for the measurement noise vector in (3), we have

$$\begin{aligned} l(\boldsymbol{\tau}) &= \frac{p(\boldsymbol{\tau}|H_1)}{p(\boldsymbol{\tau}|H_0)} \\ &= \exp\left[\frac{\boldsymbol{\tau}^T Q^{-1}\boldsymbol{\tau} - (\boldsymbol{\tau}-\tilde{\boldsymbol{\tau}})^T \boldsymbol{Q}^{-1}(\boldsymbol{\tau}-\tilde{\boldsymbol{\tau}})}{2}\right] \\ &= \exp\left[\frac{2\boldsymbol{\tau}^T \boldsymbol{Q}^{-1}\tilde{\boldsymbol{\tau}} - \tilde{\boldsymbol{\tau}}^T \boldsymbol{Q}^{-1}\tilde{\boldsymbol{\tau}}}{2}\right]. \end{aligned} \tag{10}$$

This means that (7) can be equivalently written as

$$\tilde{\boldsymbol{\tau}}^T \boldsymbol{Q}^{-1}\tilde{\boldsymbol{\tau}} - 2\boldsymbol{\tau}^T \boldsymbol{Q}^{-1}\tilde{\boldsymbol{\tau}} + 2\log\eta \underset{H_0}{\overset{H_1}{\lesseqgtr}} 0. \tag{11}$$

Let $\lambda = 2\log\eta$, (11) can be denoted by

$$\begin{bmatrix} \tilde{\boldsymbol{\tau}} \\ 1 \end{bmatrix}^T \begin{bmatrix} \boldsymbol{Q}^{-1} & -\boldsymbol{Q}^{-1}\boldsymbol{\tau} \\ -\boldsymbol{\tau}^T\boldsymbol{Q}^{-1} & \lambda \end{bmatrix} \begin{bmatrix} \tilde{\boldsymbol{\tau}} \\ 1 \end{bmatrix} \underset{H_0}{\overset{H_1}{\lesseqgtr}} 0. \tag{12}$$

Since $\tilde{\boldsymbol{\tau}}$ is the function of $\boldsymbol{u}$, the intuitive and effective decision rule for arbitrary location $\boldsymbol{u}$ of the unknown emitter can be denoted by

$$\begin{bmatrix} \boldsymbol{Q}^{-1} & -\boldsymbol{Q}^{-1}\boldsymbol{\tau} \\ -\boldsymbol{\tau}^T\boldsymbol{Q}^{-1} & \lambda \end{bmatrix} \underset{H_0}{\overset{H_1}{\lesseqgtr}} 0. \tag{13}$$

By using Schur complement, we have

$$\begin{bmatrix} \boldsymbol{Q}^{-1} & -\boldsymbol{Q}^{-1}\boldsymbol{\tau} \\ -\boldsymbol{\tau}^T\boldsymbol{Q}^{-1} & \lambda \end{bmatrix} > 0 \iff \boldsymbol{\tau}^T\boldsymbol{Q}^{-1}\boldsymbol{\tau} < \lambda \tag{14}$$

to decide that $H_0$ is true, *i.e.*, the target is absent. According to (14), we see that the decision region for $H_0$ is determined by $\boldsymbol{\tau}^T\boldsymbol{Q}^{-1}\boldsymbol{\tau} < \lambda$. Since the detection we addressed is the binary hypothesis testing problem, we can choose $\boldsymbol{\tau}^T\boldsymbol{Q}^{-1}\boldsymbol{\tau} \geq \lambda$ as the decision region for $H_1$.

## 3. THRESHOLD FOR THE NEYMAN-PEARSON TEST

As we know, the *a priori* probabilities for $H_0$ and $H_1$ are usually unknown, we adopt the Neyman-Pearson test for the detection, where the desired threshold $\lambda$ is chosen under the given constant false alarm probability (CFAR):

$$\begin{aligned} P_F &= P(H_1|H_0) = \int_{Z_1} p(\boldsymbol{\tau}|H_0) d\boldsymbol{\tau} \\ &= \int_{\boldsymbol{\tau}^T\boldsymbol{Q}^{-1}\boldsymbol{\tau}>\lambda} \frac{1}{(2\pi)^{\frac{M-1}{2}}|\boldsymbol{Q}|^{\frac{1}{2}}} \exp\left[-\frac{\boldsymbol{\tau}^T\boldsymbol{Q}^{-1}\boldsymbol{\tau}}{2}\right] d\boldsymbol{\tau}. \end{aligned} \tag{15}$$

For simplicity and without loss of generality, we first consider $M = 5$. Let

$$\boldsymbol{y} = \boldsymbol{Q}^{-\frac{1}{2}}\boldsymbol{\tau},$$

we have

$$\begin{aligned} P_F =& P(H_1|H_0) = 1 - P(H_0|H_0) \\ =& 1 - \int_{\boldsymbol{\tau}^T\boldsymbol{Q}^{-1}\boldsymbol{\tau}<\lambda} \frac{1}{(2\pi)^{\frac{5-1}{2}}|\boldsymbol{Q}|^{\frac{1}{2}}} \exp\left[-\frac{\boldsymbol{\tau}^T\boldsymbol{Q}^{-1}\boldsymbol{\tau}}{2}\right] d\boldsymbol{\tau} \\ =& 1 - \frac{1}{(2\pi)^2} \int_{\boldsymbol{y}^T\boldsymbol{y}<\lambda} \exp\left[-\frac{\boldsymbol{y}^T\boldsymbol{y}}{2}\right] d\boldsymbol{y} \\ =& 1 - \frac{1}{(2\pi)^2} \times \\ & \int_{-\sqrt{\lambda}}^{\sqrt{\lambda}} e^{-\frac{y_1^2}{2}} \left[\int_{y_2^2+y_3^2+y_4^2<\lambda-y_1^2} e^{-\frac{y_2^2+y_3^2+y_4^2}{2}} dy_4 dy_3 dy_2\right] dy_1. \end{aligned}$$

Using spherical coordinates notation, we can have

$$\begin{aligned} &\int_{y_2^2+y_3^2+y_4^2<\lambda-y_1^2} e^{-\frac{y_2^2+y_3^2+y_4^2}{2}} dy_4 dy_3 dy_2 \\ =& \int_0^{2\pi}\int_0^{\pi}\int_0^{\sqrt{\lambda-y_1^2}} e^{-\frac{r^2}{2}} r^2 \sin\varphi \, dr d\varphi d\theta \\ =& 2\pi \times \int_0^{\pi} \sin\varphi d\varphi \int_0^{\sqrt{\lambda-y_1^2}} r^2 e^{-\frac{r^2}{2}} dr \\ =& 4\pi \times \int_0^{\sqrt{\lambda-y_1^2}} r^2 e^{-\frac{r^2}{2}} dr, \end{aligned}$$

such that

$$\begin{aligned} P_F &= 1 - \frac{4\pi}{(2\pi)^2} \int_{-\sqrt{\lambda}}^{\sqrt{\lambda}} e^{-\frac{y_1^2}{2}} \int_0^{\sqrt{\lambda-y_1^2}} r^2 e^{-\frac{r^2}{2}} dr dy_1 \\ &= 1 - \frac{1}{2\pi} \int_{-\sqrt{\lambda}}^{\sqrt{\lambda}} \int_{-\sqrt{\lambda-y_1^2}}^{\sqrt{\lambda-y_1^2}} r^2 e^{-\frac{r^2+y_1^2}{2}} dr dy_1. \end{aligned} \tag{16}$$

Similarly, let
$$\begin{cases} y_1 = \rho\cos\phi \\ r = \rho\sin\phi \end{cases}$$
then we obtain

$$\begin{aligned} P_F &= 1 - \frac{1}{2\pi}\int_0^{2\pi}\int_0^{\sqrt{\lambda}} \rho^2 \sin^2\phi e^{-\frac{\rho^2}{2}} \rho d\rho d\phi \\ &= 1 - \frac{1}{4\pi}\int_0^{2\pi}(1-\cos 2\phi)d\phi \int_0^{\sqrt{\lambda}} \rho^3 e^{-\frac{\rho^2}{2}} d\rho \\ &= \frac{1}{2}e^{-\frac{\lambda}{2}}(\lambda+2). \end{aligned} \tag{17}$$

Using the similar derivation steps for the case of $M = 5$, we can obtain the results for $M = 6$ and $M = 7$:

$$P_F = 1 - erf\left(\sqrt{\frac{\lambda}{2}}\right) + \sqrt{\frac{2}{9\pi}}e^{-\frac{\lambda}{2}}\left(\left(\sqrt{\lambda}\right)^3 + 3\sqrt{\lambda}\right) \tag{18}$$

and
$$P_F = \frac{1}{8}e^{-\frac{\lambda}{2}}(\lambda^2 + 4\lambda + 8) \tag{19}$$

respectively, where $erf(x)$ is the error function defined by $erf(x) = \int_0^x e^{-t^2}dt$.

The desired threshold for the Neyman-Pearson test can thus be obtained by solving (17), or (18), or (19).

## 4. DETECTION AND LOCALIZATION USING TDOA MEASUREMENTS AND SPARSITY

From the point of view of surveillance, we care not only the presence/absence of the unknown emitter, but also the location of the emitter in the interested (concerned) area if it was present. According to the measurement model (1), the maximum likelihood localization (MLL) for unknown emitter is straightforwardly denoted by

$$\min_{\boldsymbol{u}} \sum_{i=2}^{M}\left(\frac{1}{c}||\boldsymbol{u}-\boldsymbol{s}_i|| - \frac{1}{c}||\boldsymbol{u}-\boldsymbol{s}_1|| - \tau_{i1}\right)^2 \tag{20}$$

which can be equivalently written as

$$\begin{aligned} \min_{\boldsymbol{u},\boldsymbol{t}} \quad & \sum_{i=2}^{M}(t_i - t_1 - \tau_{i1})^2 \\ \text{subject to} \quad & \frac{1}{c}||\boldsymbol{u}-\boldsymbol{s}_i|| = t_i, \quad i = 1,\ldots,M. \end{aligned} \tag{21}$$

Since the location of the unknown emitter is a (sparse) point in the interested area, it is natural to consider dividing the interested area into a number of small space cells. For instance, we divide the interested area into $H\times L\times W$ cubic cells [$H$ is the number in height, $L$ is the number in length, and $W$ is the number in width] and denote $\boldsymbol{u}_i \in \mathcal{R}^3$ as the center location of the $i$th cell, the MLL (21) can be reformulated under the framework of support detection [5]

$$\begin{aligned} \min_{\boldsymbol{x},\boldsymbol{t}} \quad & \sum_{i=2}^{M}(t_i - t_1 - \tau_{i1})^2 + \lambda||\boldsymbol{x}||_1 \\ \text{subject to} \quad & \frac{1}{c}||\boldsymbol{U}\boldsymbol{x}-\boldsymbol{s}_i|| = t_i, \\ & \boldsymbol{x} \geq 0, \ \ i = 1,\ldots,M \end{aligned} \tag{22}$$

where $\boldsymbol{U} = [\boldsymbol{u}_1,\ldots,\boldsymbol{u}_{HLW}] \in \mathcal{R}^{3\times HLW}$, $\boldsymbol{x} \in \mathcal{R}^{HLW\times 1}$ is a sparse vector with very few elements (or one element) greater than zero, and $\lambda$ $(> 0)$ is a proper parameter to keep the sparsity of $\boldsymbol{x}$. It is seen that (22) is a non-linear and nonconvex optimization problem. By relaxing the equality constraints in (22) to inequality ones, the optimization problem (22) can be cast into the following convex programming:

$$\begin{aligned} \min_{\boldsymbol{x},\boldsymbol{t}} \quad & \sum_{i=2}^{M}(t_i - t_1 - \tau_{i1})^2 + \lambda||\boldsymbol{x}||_1 + \delta\sum_{i=1}^{M} t_i^2 \\ \text{subject to} \quad & \frac{1}{c}||\boldsymbol{U}\boldsymbol{x}-\boldsymbol{s}_i|| \leq t_i, \\ & \boldsymbol{x} \geq 0, \ \ i = 1,\ldots,M \end{aligned} \tag{23}$$

where $\delta$ is a positive constant for penalization ranging from $10^{-8}$ to $10^{-4}$. (23) can be solved by *SeDuMi*, an efficient solver for convex optimization problems. By solving (23), we have the solution $\boldsymbol{x}$ and then the emitter location estimate $\hat{\boldsymbol{u}} = \boldsymbol{U}\boldsymbol{x}$, which can be refined by applying any standard nonlinear optimization routine to (20).

## 5. NUMERICAL RESULTS

We here conduct three computer simulations to state the the receiver operating characteristics (ROC) of the abovementioned detection methods. In the first simulation, we consider the impact of the number of employed sensor nodes for detection on the ROC performance, where detection is performed by the decision rule of (13) with the threshold (17), (18), and (19), respectively. The second simulation focuses on the ROC for the cases where the unknown emitter locates in either the near field, or far field of the interested area, or outside the area, where $M = 5$ nodes are employed, following the decision rule of (13) with the threshold (17). Moreover, the results by solving (23) are involved in the detection when $H_1$ is declared to be true. To make tradeoff between the performance and the energy used for data transmission, in the third simulation we evaluate impact of the length of the received signal samples for cross-correlation on the ROC performance, where the process of decision is the same as that in the second simulation. Without loss of generality, we assume that the unknown emitter transmits QPSK signals and its signal bandwidth is 10MHz. For all the simulations, $8\times 10^7$ Monte Carlo runs are performed to evaluate the ROC performance for each case. In all the simulations, even neighboring nodes or a portion of them are involved in the detection process, whose locations are listed in Table I.

**Table 1**. Locations of the Sensor Nodes

| node no. | 1 | 2 | 3 | 4 | 5 | 6 | 7 |
|---|---|---|---|---|---|---|---|
| $x$ | 0 | 879 | 0 | -990 | 1023 | -1327 | 0 |
| $y$ | 0 | 0 | 1115 | -1220 | 887 | 0 | -925 |
| $z$ | 5 | 15 | 20 | 10 | 4 | 13 | 18 |

*Simulation #1:* In this simulation, the location of the unknown emitter and the covariance matrix of the TDOA measurement noise [6] are respectively set to $\boldsymbol{u}^0 = [700, 800, 750]^T$ and

$$\boldsymbol{Q} = \sigma_n^2 \begin{bmatrix} 1 & 1/2 & \ldots & 1/2 \\ 1/2 & 1 & \ldots & 1/2 \\ \vdots & \vdots & \ddots & \vdots \\ 1/2 & 1/2 & \ldots & 1 \end{bmatrix}_{(M-1)\times(M-1)}$$

where $\sigma_n = 3\times 10^{-8}$ (s). According to the definition for $P_F$ and $P_D$ by (8) and (9), the ROC curves are plotted in Fig.1 for the cases where the first $M = 4, 5, 6, 7$ sensor nodes listed in Table I are respectively employed for detection. For comparison, the corresponding theoretical ROC curves without marks are plotted in the figure.

From Fig.1, we see that more sensor nodes employed result in more performance improvement.

*Simulation #2:* In this simulation, we consider the effect of the propagation loss on performance. We denote $d_i$ as the distance between $i$-th sensor and the emitter. For simplicity and without loss of generality, we set the unknown emitter location to $\boldsymbol{u}^0 = [700, 800, 750]^T$ for near-filed case and consider the $d_0 = \| [700, 800, 750]^T - [0, 0, 5]^T \|$ as the reference, the received signal to noise ratio of the $i$-th sensor is scaled by $d_0^2/d_i^2$. The TDOA measurements are obtained by performing crosscorrelation between the 1st sensor and the $i$-th ($i = 2, \ldots, M$) sensor, where the sampling frequency is set to 100MHz and 200 received signal samples at the cluster head are broadcast. Furthermore, we set the unknown emitter location to $\boldsymbol{u}^0 = [1600, 1700, 1500]^T$ for the far-field case, while $\boldsymbol{u}^0 = [4800, 4800, 4800]^T$ outside the interested area. The interested area is assumed with the height from 100m to 4000m, the length from $-4000$m to 4000m, and the width from $-4000$m to 4000m. We employ $M = 5$ sensor nodes for detection, and the SNR of the received signal at the reference sensor node located at $[0, 0, 5]^T$ is considered as $-1$db for the near-field case. In Fig.2, we plotted the ROC curves for these three cases. From the figure, it is seen that the detection performance decreases significantly with the increase of the distance between the sensors and the emitter.

*Simulation #3:* In this simulation, we consider the effect of three different numbers of received signal samples on ROC performance, which are broadcast to the neighboring nodes. These numbers of samples are corresponding to the same time duration. This is to say, the received signals are sampled by different sampling frequency. Here we adopt 100, 200, and 400 samples corresponding to sampling frequency 50MHz, 100MHz, and 200MHz, respectively. The location of the unknown emitter is assumed as $\boldsymbol{u}^0 = [700, 800, 750]^T$, and $M = 5$ sensor nodes are employed. The SNR of the received signal at the cluster head node (located at $[0, 0, 5]^T$) is considered as 0db. The corresponding ROC curves are plotted in Fig.3. From the figure, we see that the more samples in the same duration are broadcast, *i.e.*, the higher sampling frequency is used, the better the performance will be. The tradeoff on the number of the samples will be made according to the practical performance requirements.

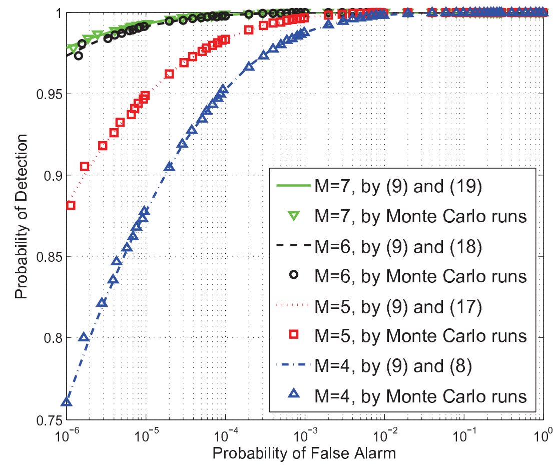


**Fig. 1**. ROC versus the number of sensor nodes $M$

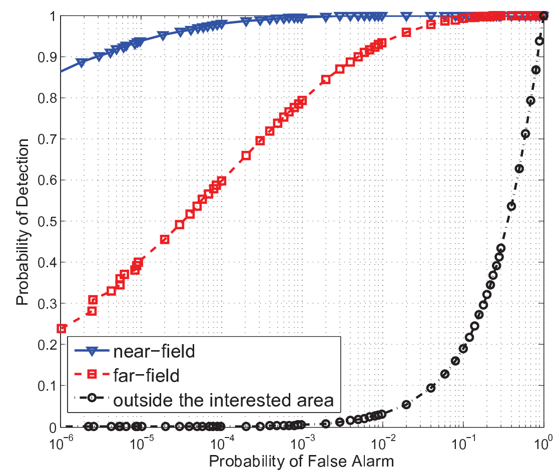


**Fig. 2**. ROC versus the unknown emitter location

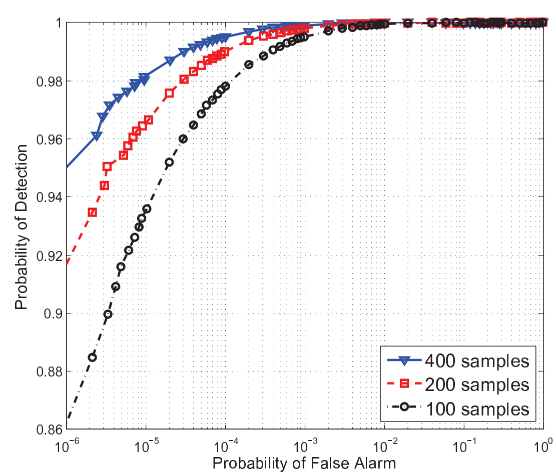


**Fig. 3**. ROC versus the number of received signal samples

## 6. REFERENCES


[1] K. Yang, G.Wang, and Z.-Q. Luo, "Efficient Convex Relaxation Methods for Robust Target Localization by a Sensor Network Using Time Differences of Arrials", *IEEE Trans. Signal Process.*, vol. 57, pp. 2775-2784, Jul. 2009.

[2] J. N. Tsitsiklis, "Decentralized detection," in *Advances in Statistical Signal Processing, Vol. 2: Signal Detection*, H. V. Poor and J. B. Thomas, Eds. Greenwich, CT: JAI, 1990.

[3] P. K. Varshney, *Distributed Detection and Data Fusion*, New York: Springer-Verlag, 1997.

[4] Y. Wang and W. Yin, "Sparse signal reconstruction via iterative support detection," *SIAM Journal on Imaging Sciences.*, vol. 3, no. 3, pp. 462-491, 2010.

[5] Q. Ling and Z. Tian, "Decentralized Support Detection of Multiple Measurement Vectors with Joint Sparsity," *Proc. of IEEE International Conference on Acoustics, Speech and Signal Processing (ICASSP)*, May 2011, pp. 2996-2999.

[6] Y.-T. Chan and K. C. Ho, "A simple and efficient estimator for hyperbolic location," *IEEE Trans. Signal Process.*, vol. 42, pp. 1905-1915, Aug. 2006.